

# NEUTRINO PHYSICS

Alexei Yu. Smirnov

International Centre for Theoretical Physics, Trieste, Italy and

Institute for Nuclear Research, Moscow, Russia

## Abstract

Flavors, masses and mixing of neutrinos are introduced. We consider properties of propagation of mixed neutrinos in vacuum and matter. We describe status and solutions of the solar and atmospheric neutrino problems and also discuss some other hints to non zero neutrino mass. Possible patterns of neutrino masses and mixing are presented.

## 1. INTRODUCTION

The lectures are devoted to the problem of neutrino masses and lepton mixing. After the top quark discovery the neutrinos are the only known fermions with unknown masses. Massive neutrinos may have a number of crucial implications to astrophysics and cosmology (evolution of the Universe, structure formation, nucleosynthesis, star evolution). Knowledge of neutrino masses and mixing may shed some light on fermion mass problem, quark-lepton symmetry, B- and L- number non-conservation, existence and properties of new mass scales.

## 2. FLAVORS, MASSES, MIXING

To set notations we recall on basic notions concerning neutrino flavors, masses and mixing.

### 2.1 Neutrino flavors

The electron,  $\nu_e$ , muon,  $\nu_\mu$ , and tau,  $\nu_\tau$ , neutrinos are defined as the states which form charge currents with electron, muon, and tau lepton correspondingly:

$$J^\mu = \bar{\nu}_l \gamma^\mu (1 - \gamma_5) l, \quad l = e, \mu, \tau. \quad (1)$$

Equivalently, one can say that  $\nu_l$  form the SU(2)-doublets of the Standard Model (SM), with lepton  $l$ . The states  $\nu_e$ ,  $\nu_\mu$  and  $\nu_\tau$ , are called the flavor states (in contrast with quark sector, where flavors are identified with states having definite masses).

Phenomenologically,  $\nu_e$  is defined as the state produced together with positron,  $\nu_\mu$  - as the state interacting with muon, etc. In general, these two definitions do not coincide. Moreover, the phenomenological definition is process-dependent. Plausible situation is when light (or massless) neutrinos,  $\tilde{\nu}_l$ , are mixed with heavy leptonic states,  $N_l$  in the charged current, so that

$$\nu_l = \sqrt{1 - \epsilon_l^2} \tilde{\nu}_l + \epsilon_l N_l. \quad (2)$$

If the mass of heavy lepton is bigger than the energy release in a given process than phenomenological neutrino will be identified with  $\tilde{\nu}_l$ , and obviously,  $\nu_l \neq \tilde{\nu}_l$ . Moreover, the phenomenological electron neutrino may not be orthogonal to phenomenological muon (or tau) neutrino:

$$\langle \tilde{\nu}_e | \tilde{\nu}_\mu \rangle = -\epsilon_e \epsilon_\mu \langle N_e | N_\mu \rangle. \quad (3)$$

The nonorthogonality (3) is a manifestation of the lepton number violation. In fact, such a situation can be realized in the sea - saw mechanism [2, 3], where  $N_l$  are the right handed Majorana neutrinos and  $\epsilon_l \sim m_D/M_N$ . Here  $m_D$  is the Dirac mass of neutrino. In the most appealing scenario masses of heavy leptons are at the intermediate scale,  $m_N = 10^{10} - 10^{12}$  GeV, or even at the Grand Unification (GU) scale. And the admixture parameter is typically of the order  $\epsilon \sim v_{EW}/m_N$ , *i.e.* too small to be detected in experiment.

For the so called electroweak see - saw characterized by  $m_N \sim G_F^{-1/2}$ , a violation of the universality could be observable. There is another example. Suppose that  $\nu_3$  has tau flavor and its mass is in MeV region. Then it can not be produced in beta decay, therefore  $\nu_3$  will play the role of  $N_l$ .

## 2.2 Number of neutrino flavors

Neutrino channel,  $Z \rightarrow \nu \bar{\nu}$ , contributes to the invisible width of  $Z$ -decay:  $\Gamma_{inv} = \Gamma_{tot} - \Gamma_l - \Gamma_h$ , where  $\Gamma_{tot}, \Gamma_l, \Gamma_h$  are the total, (charge) lepton and hadron widths. The effective number of neutrino species is defined as  $N_\nu = \frac{\Gamma_{inv}}{\Gamma_\nu}$ , where  $\Gamma_\nu$  is the neutrino width in the Standard Model. The LEP data give [1] (fit of the Z - line shape)

$$N_\nu = 2.987 \pm 0.012 \quad (4)$$

in agreement with expected 3. In the analysis it was assumed that three neutrino-anti-neutrino pairs  $\nu_e \bar{\nu}_e$ ,  $\nu_\mu \bar{\nu}_\mu$ ,  $\nu_\tau \bar{\nu}_\tau$  are produced independently and their widths sum in the total (invisible) width. This is correct if lepton numbers,  $L_e, L_\mu, L_\tau$ , are conserved. However, if lepton numbers are broken and neutrinos mix it is more natural to consider a production of pairs with definite masses:  $\nu_i \bar{\nu}_i$ , ( $i = 1, 2, 3$ ) in  $Z$ -decay. As follows from the Lagrangian of the SM, the state which appears in  $Z$ -decay is [4]

$$|\nu_Z\rangle = \frac{1}{\sqrt{3}} [|\bar{\nu}_1\rangle|\nu_1\rangle + |\bar{\nu}_2\rangle|\nu_2\rangle + |\bar{\nu}_3\rangle|\nu_3\rangle]. \quad (5)$$

This state gives the same invisible width of Z as three independent flavor pairs:

$$\Gamma \propto |\langle \nu_Z | H | Z^0 \rangle|^2 = 3 \left( \frac{g}{2} \right)^2. \quad (6)$$

The physical difference of the state (5) and independent pairs is that  $\nu_Z$  is the coherent state and one can observe oscillations in this state provided both neutrino and antineutrino components are detected [4].

Another source of information on the number of neutrino species is the Primordial nucleosynthesis [10].

### 2.3 Dirac and Majorana neutrinos

In the Standard Model:  $m_\nu = 0$ . This follows from the content of the model, namely, from the fact that in the model there is

- no right handed neutrino components,
- no Higgs triplets which can give the Majorana mass for the left handed neutrinos.

The absence of the  $\nu_R$  gives an explanation of strong upper bounds on the neutrino masses. However, it looks rather unnatural. In particular, this implies that the left-right symmetry does not appear at any level.

Moreover, both above items can be questioned by gravity.

If there are the right handed neutrinos,  $\nu_R$ , one can introduce the Dirac mass term

$$-m_D(\bar{\nu}_L\nu_R + \bar{\nu}_R\nu_L) \quad (7)$$

which has the weak isospin 1/2 and can be generated by Yukawa coupling with Higgs doublet.

To construct a mass term one can use the charge conjugated state of  $\nu_L$ :  $(\nu_L)^c \equiv C(\bar{\nu}_L)^T$  (where  $C \equiv i\gamma^2\gamma^0$ ) instead of  $\nu_R$ :

$$-\frac{m}{2}(\bar{\nu}_L\nu_R^c + \bar{\nu}_R^c\nu_L). \quad (8)$$

The term (8) can be rewritten as

$$\pm\frac{m}{2}(\bar{\nu}_M\nu_M), \quad (9)$$

where  $\nu_M = \nu_L \pm (\nu_L)^c$ . The state  $\nu_M = \nu_L \pm (\nu_L)^c$  has the property

$$\nu_M = \pm(\nu_M)^c, \quad (10)$$

*i.e.* turns out to be true neutral (Majorana) neutrino. The Majorana mass term (8) carry the lepton number  $|\Delta L| = 2$ , and consequently, leads to the processes with lepton number violation by two units. The sign in (10) (related to the sign of the mass in (9)) determines the CP-parity of the neutrino state.

The Majorana mass term has the weak isospin  $I = 1$  and can be generated by the effective operator

$$\frac{1}{M}LLHH, \quad (11)$$

where  $L$  is the lepton doublet and  $H$  is the Higgs doublet. Mass parameter  $M$  characterizes the scale at which the operator (11) is formed.

The operator (11) can be generated by renormalizable interaction with exchange of particle having mass  $M$  as it happens in the see-saw mechanism. It can be produced radiatively which implies some physics beyond the SM. However, it may appear in the SM immediately due to gravitational effects, so that  $M = M_P$ , where  $M_P$  is the Planck mass.

An alternative possibility is that a theory contains Higgs triplet  $\Delta$  ( $I = 1$ ) and there is the interaction  $LL\Delta$ , so that the VEV of  $\Delta$  generates the mass term (8).

## 2.4 Mixing

If neutrinos are massive they (most probably ) mix. This statement is based on analogy with quark sector. It is difficult to explain an absence of mixing of massive neutrinos. Thus, flavor states  $\nu_f \equiv (\nu_e, \nu_\mu, \nu_\tau)$  do not coincide with mass states  $\nu_m \equiv (\nu_1, \nu_2, \nu_3)$ . Mass states are mixtures (combinations) of the flavor states and *vice versa*. Flavor states are related to the mass states by the unitary (mixing) matrix  $U$ :

$$\nu_f = U \nu_m. \quad (12)$$

In the two neutrino case:

$$\nu_e = \cos \theta \nu_1 + \sin \theta \nu_2, \quad \nu_\mu = \cos \theta \nu_2 - \sin \theta \nu_1, \quad (13)$$

where  $\theta$  is the mixing angle.

## 2.5 Bounds on neutrino masses from direct searches and the $\beta\beta_{0\nu} - \text{decay}$

The bounds on neutrino masses are summarized in Fig. 1. Several comments are in order.

### 1. *Electron neutrino*

The measurement of the electron energy spectrum (Curie plot) in the decay  ${}^3H \rightarrow {}^3He + e^- + \bar{\nu}_e$  near the end point is the most sensitive to the neutrino mass. The best bound have been obtained in INR RAS (Moscow) experiment with integral electrostatic spectrometer [6]. ‘‘Conditional’’ bound is

$$m(\nu_e) < 3.5 \text{ eV} \quad 95\% \text{ C.L. .}$$

It should be noted however, that the results of the experiment have some unexplained features: in particular, there is a flat excess in the integral energy spectrum which starts very close to the end point. It is this feature leads to the negative value of the  $m^2$  in usual fit. The excess corresponds to the peak in the differential spectrum, and the result (2.5) has been obtained by subtraction of the peak.

It turns out that a position of the peak depends on conditions of the experiment. In the run of experiment in 1994 the peak was at  $Q - E_e \approx 7 \text{ eV}$ , whereas in the run 1996 the peak is at  $Q - E_e \sim 11 \text{ eV}$ . There were some changes of the experiment in the run 1996, in particular, the strength of the magnetic field was higher. The shift of the peak indicates that it has an instrumental origin, rather than origin in neutrino properties (the tachionic nature of neutrinos, or the existence of dense degenerate neutrino sea). In fact, this justifies the subtraction of the excess.

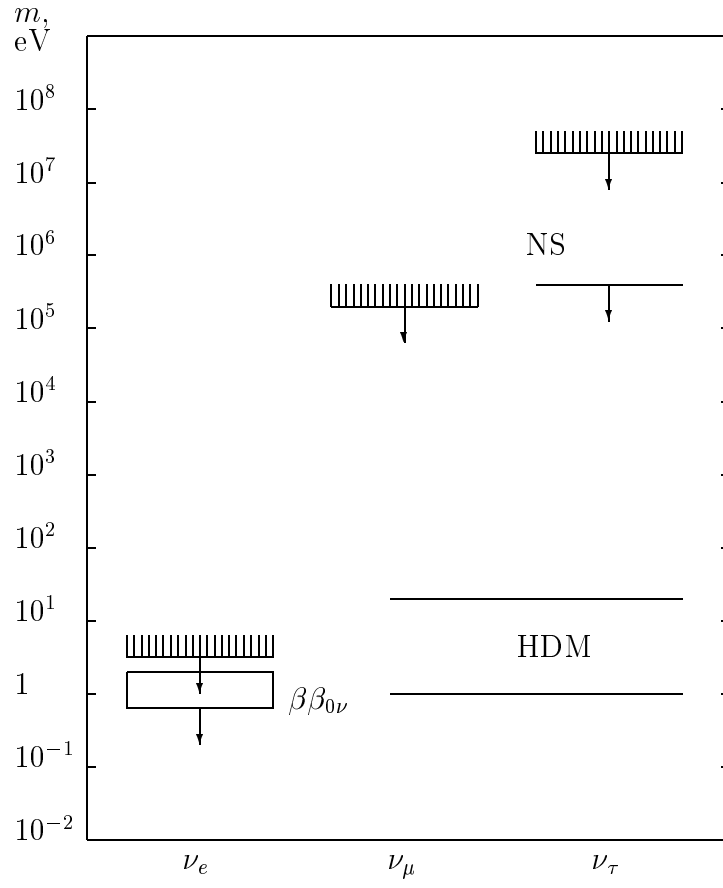


Fig. 1. Bounds on neutrino mass from direct searches and neutrinoless double beta decay. Also shown are the bound on the mass of long-lived neutrino from primordial nucleosynthesis (NS) and the range of the hot dark matter neutrino masses (HDM).

Similar experiment in Mainz has given the bound [7]:  $m < 7.2$  eV at 95% C.L. .

There is another feature in the spectrum: the excess of events at lower energies of the electrons:  $Q - E_e \gtrsim 200$  eV. Similar excess was also observed by Mainz group. One possible explanation of this anomaly is an existence of neutrino with mass  $m \sim 200$  eV whose admixture in the electron neutrino state is characterized by probability  $P \sim 1 - 2\%$ . This is precisely in the range implied by pulsar velocities (see sect. 4.3).

2. Measurements of the momentum of muon from the pion decay at rest in PSI (Switzerland) [8] and the mass of pion give kinematical bound on the mass of muon neutrino

$$m(\nu_\mu) < 0.16 \text{ MeV}, \quad 90\% \text{ C.L. .}$$

3. For tau neutrino the best bound follows from studies of decays of  $\tau$ -leptons:

$$\tau \rightarrow 5\pi(\pi^0)\nu_\tau . \quad (14)$$

ALEPH collaboration (LEP, CERN  $e^+e^-$  - collisions,  $Z \rightarrow \tau^- + \tau^+$  -decay) has measured the hadron energy and the invariant mass of pions. This gives the two dimensional distribution of events. The existence of the events with the energy and the invariant mass near the end point leads to the limit [9]

$$m(\nu_\tau) < 23 \text{ MeV} , \quad 95\% \text{ C.L. .} \quad (15)$$

The limit could be relaxed if one admits mixing of the tau neutrino with muon neutrino, so that in  $\nu_\tau$  there is some small admixture of the light state.

Strong bound follows from the primordial nucleosynthesis (see [10] for review).

4. *Double beta decay.* Majorana mass of the electron neutrino is restricted by the neutrinoless double beta decay  $Z \rightarrow (Z + 2) + 2e^-$ . For  $m \ll 1/r_N \sim p \sim 30$  MeV, where  $p$  is typical momentum of particle within the nuclei, the amplitude of the decay is proportional to:

$$A \propto \left\langle \frac{m}{p^2} \right\rangle_N . \quad (16)$$

Here  $\langle \dots \rangle_N$  is the nuclear matrix element. A distinctive property of the decay is that the sum of energies of two electrons is fixed by mass difference of initial and final nuclei, *i.e.* the spectrum is monochromatic.

The best limit has been obtained by Heidelberg-Moscow collaboration for the decay  $^{76}\text{Ge} \rightarrow ^{76}\text{Se} + 2e^-$ . The experiment is performed with enriched  $^{76}\text{Ge}$  isotope in the Laboratory Gran-Sasso. Lower bound for the half life time corresponds to the upper bound on the electron neutrino mass [11]

$$m < 0.68 \text{ eV} , \quad 90\% \text{ C.L. ,} \quad (17)$$

for matrix element calculated in [12]). The uncertainties in the nuclear matrix element could be estimated by factor 2, and more conservative bound is  $m < 1$  eV.

Vacuum neutrino mixing may influence the double beta decay. The neutrinoless double beta decay is determined by  $m_{ee}$  element of neutrino mass matrix (if all neutrino

masses  $m_i \ll 30$  MeV). In terms of mass eigenstates the effective mass of the electron neutrino,  $m_{ee}$ , can be written as

$$m_{ee} = \sum_i U_{ei}^2 \cdot m_i, \quad (18)$$

where  $U_{ei}$  is the element of the mixing matrix  $S$ . In this connection two points should be stressed.

- Neutrino masses can be both positive and negative which corresponds to different CP-parities (8). Therefore for different signs one may have partial or complete cancellation in (18). In this case the restriction (17) does not exclude masses up to kinematical bound 3.5 eV. (A complete compensation takes place for a system of two Majorana neutrinos with  $m_1 = -m_2$  and  $U_{e1} = U_{e2}$ . The system evidently has a symmetry which is the symmetry of lepton number. In fact, these two Majorana components form Dirac neutrino.
- If there is no cancellation and one of neutrino components dominates in the sum (18), the double beta decay bound (17) restricts admixture of this dominant component in the electron neutrino:

$$|U_{ei}| < \sqrt{\frac{m_{ee}}{m_i}}. \quad (19)$$

For  $m_3 \sim 20$  MeV we get  $|U_{e3}| < 1.6 \cdot 10^{-4}$  which is at least one order of magnitude smaller than corresponding mixing in quark sector ( $V_{td}$ ). For  $m_2 = 160$  keV Eq. (19) gives  $|U_{e2}| < 1.8 \cdot 10^{-3}$  which is much smaller than Cabibbo angle. These restrictions are important for the electroweak see-saw. Note that the bound (17) is stronger than the mass needed to explain HDM in the Universe.

5. Lower bound on neutrino mass? For  $M = M_P$ , we get from (11)

$$m_{\nu P} \sim \frac{\eta \langle H \rangle^2}{M_P} \sim 10^{-5} \text{ eV} , \quad (20)$$

where  $\eta \sim 1$  is the renormalization group factor. The value (20) can be considered as the lower bound on neutrino mass. Indeed,  $M_P$  is the largest mass scale we have in the theory. If some new interactions exist below this scale at  $M < M_P$ , they can generate neutrino mass,  $\eta \langle H \rangle^2 / M$ , larger than  $m_{\nu P}$ . Inverting the point, one can say that observation of mass  $m_\nu > m_{\nu P}$  will testify for new physics below the Planck scale:

$$M \sim \frac{1}{G_F m_\nu} . \quad (21)$$

Physical scale (the scale of new particle masses, or condensates) can be even much smaller than the one estimated from (21). In particular,  $M$  can be a combination of other mass parameters  $M'$ ,  $m_{3/2}$  etc. (where  $m_{3/2}$  is the gravitino mass) which are much smaller than  $M$  itself: *e.g.*  $M = (M')^2 / m_{3/2}$ .

A phenomenological lower bound on  $m_\nu$  has been suggested recently [13]. The exchange of massless neutrinos leads to the long range neutrino forces. In particular, two body potential due to the exchange of the  $\bar{\nu}\nu$  - pair gives [14] :

$$V_0^{(2)} = \frac{a G_F^2}{4\pi^3 r^5} , \quad (22)$$

where  $a$  is known coefficient. Many body (four, six ...  $k$  ...) potentials contain additional factors  $(G_F/r^2)^{2k}$  which are extremely small for macroscopic  $r$ . However in compact stellar objects like neutron stars and white dwarfs, the contributions of these many body interactions to energy of the star are greatly enhanced due to combinatorial factor.

The contribution of  $k$ -body interactions,  $W^k$ , to the total energy is proportional to number of combinations of  $k$ -neutrons from total number of neutrons in a star. The combinatorial factor leads to the series parameter  $W^{k+2}/W^k \sim (G_F n R_{ns})^2 \sim (10^{13})^2$ , where  $n$  is the number density of neutrons and  $R_{ns}$  is the radius of neutron star. So that, the six body contribution to the energy dominates over the four body contribution *etc.* [13]. It turns out that the energy due to the eight body interactions overcomes the mass of a star. According to [13] the only way to resolve this paradox is to assume that all neutrinos have nonzero masses:  $m_\nu > 0.4$  eV. Neutrino mass cuts off the forces at  $r > 1/m_\nu$ .

There is, however, another resolution of the paradox and the mass of neutrino still can be zero.

The series over  $k$  are divergent but they are alternative. It was shown that another procedure of resummation of series over the  $k$ -body interactions leads to very small total energy [15].

Stars form unusual systems in which  $n$ -body forces dominate over  $n - 1$  body forces. There is, however, physical reason which can make the series to be convergent.

Indeed, a star can be considered as a potential well with the depth  $V \sim G_F n$ , where  $V$  is due to neutrino interactions with particles of medium,  $G_F$  is the Fermi constant,  $n$  is the number density of the particles. The potential has different signs for neutrinos and antineutrinos. Therefore, neutrinos are trapped, whereas antineutrinos are expelled from the star. In such a way strongly degenerate sea is formed [16].

The degenerate sea in stars leads to Pauli blocking of the long range forces [17]. As the result the many body forces do not dominate in self energy of star. This can resolve the energy paradox suggested in [13] even for massless neutrinos [17].

### 3. NEUTRINO PROPAGATION IN VACUUM AND MATTER

There are two different effects of the propagation of mixed neutrinos (see reviews [18], [19]):

- 1). Oscillations which take place (in pure form) in vacuum or in uniform medium.
- 2). Resonance conversion which may occur in medium with monotonously changing density.

Although both oscillation and conversion require mixing and are consequences of mixing these are two different effects. Resonance conversion is not the enhanced oscillations. In fact, in the non-uniform medium one expects an interplay of both processes: oscillations and resonance conversion.

#### 3.1 Oscillations

Surprisingly enough, there is a number of recent papers on theory of neutrino oscillations [20]. Basic motivation is to find the limits of application of the so called standard oscillation formula. In what follows we will reproduce the oscillation formula in a way which allows to resolve some paradoxes of the neutrino oscillations.



The oscillation effect is related to phases which the neutrino mass eigenstates acquire during propagation.

Suppose  $\nu_e$  is produced in vacuum:  $\nu(0) = \nu_e = \cos\theta\nu_1 + \sin\theta\nu_2$ . (In fact as we stressed in sect. 2.1, the neutrino state is process dependent and one should calculate  $A_i$  - the amplitudes of probabilities of production of  $\nu_i$ , ( $i = 1, 2$ ). The amplitudes coincide with  $\cos\theta$  and  $\sin\theta$  only if neutrino masses are much smaller than the energy release and there is no chirality suppression effect like a suppression in the pion decay. Mass states  $\nu_1$  and  $\nu_2$  are the eigenstates of the Hamiltonian in vacuum. This means that  $\nu_1$  and  $\nu_2$  propagate independently and there is no  $\nu_1 \leftrightarrow \nu_2$  transitions. The only what happens is that  $\nu_1$  and  $\nu_2$  acquire phases:

$$\nu_i \rightarrow \nu_i e^{i\phi_i}, \quad (23)$$

where

$$\phi_i \equiv E_i t - p_i x, \quad (24)$$

and moreover,  $\phi_1 \neq \phi_2$  due to mass difference. As the result in an arbitrary moment a neutrino state can be written as

$$\nu(t) = \cos\theta\nu_1 + \sin\theta\nu_2 e^{i\Delta\phi(t)}, \quad (25)$$

where

$$\Delta\phi \equiv \phi_2 - \phi_1 \quad (26)$$

(the common factor  $\exp(i\phi_1)$  is omitted since it has no physical sense).

Let us find  $\Delta\phi$ . The states  $\nu_i$  have no fixed momenta and energy: they are described by wave packets with some spread of momenta. Therefore in general we should consider an interference of waves with different momenta and energies. From (24) we have

$$\Delta\phi = \Delta E t - \Delta p x. \quad (27)$$

In the case of macroscopic distance between the source and detector neutrinos can be considered as being on the mass shell, so that  $E = \sqrt{p^2 + m^2}$ . Then the energy difference equals

$$\Delta E = \frac{dE}{dp} \Delta p + \frac{dE}{dm^2} \Delta m^2 = v_g \Delta p + \frac{1}{2E} \Delta m^2, \quad (28)$$

where  $v_g \equiv dE/dp$  is the group velocity and  $\Delta m^2 \equiv m_2^2 - m_1^2$  is the neutrino mass squared difference. Substituting the expression (28) into (27) we get

$$\Delta\phi = \Delta p(v_g t - x) + \frac{\Delta m^2}{2E} t. \quad (29)$$

The first term in (29) vanishes in the center of wave packet. Moreover, if spatial size of the wave packet is sufficiently small:

$$\sigma_x \ll \frac{1}{\Delta p}, \quad (30)$$

the first term in (29) can be neglected for any point of the packet ( $\Delta p(v_g t - x) < \Delta p \sigma_x \ll 1$ ). In this case we get usual expression for the phase difference

$$\Delta\phi = \frac{\Delta m^2}{2E} t. \quad (31)$$

It is this monotonous increase of the phase difference with time that results in oscillations. Indeed, according to (25) maximal deviation from the initial state is when  $\Delta\phi = \pi$ :  $\nu(\pi) = \cos\theta\nu_1 - \sin\theta\nu_2$ . The probability to find  $\nu_e$  in this state is  $P_\pi = |\langle\nu_e|\nu(\pi)\rangle|^2 = \cos^2 2\theta$ . Therefore a depth of oscillations equals

$$A_P = 1 - P_\pi = \sin^2 2\theta. \quad (32)$$

A neutrino state returns to the initial (flavor) state when  $\Delta\phi = 2\pi$ . Substituting  $\Delta\phi = 2\pi$  in (31) we get the distance

$$l_\nu \approx t_{2\pi} = \frac{4\pi E}{\Delta m^2} \quad (33)$$

which is called the oscillation length. Now we can immediately write the “standard oscillation formula” - the expression for the oscillation transition probability:

$$P_{tr} = \frac{A_P}{2} \left(1 - \cos \frac{2\pi x}{l_\nu}\right) = \sin^2 2\theta \sin^2 \frac{\pi x}{l_\nu}. \quad (34)$$

Let us come back to the condition (30). If  $\Delta p \sim \frac{\Delta m^2}{2E} = 2\pi/l_\nu$ , then it can be written as

$$\sigma_x \ll l_\nu/2\pi. \quad (35)$$

Since  $\sigma_x < \Delta L$ , where  $\Delta L$  is the size of neutrino source or detector, the above inequality is nothing but the condition of non averaging the oscillations.

Let us describe physics of oscillations in other terms. Formulas (13) can be inverted as

$$\nu_1 = \cos\theta\nu_e - \sin\theta\nu_\mu, \quad \nu_2 = \cos\theta\nu_\mu + \sin\theta\nu_e. \quad (36)$$

These equations determine the flavors, or more precisely, flavor compositions of the neutrino eigenstates  $\nu_1, \nu_2$  (the eigenstates of the Hamiltonian). According to (36) *flavors of the eigenstates are determined by mixing angle*. Mixing angle is fixed in vacuum and therefore the flavors of the eigenstates are fixed.

Summarizing we can say:

- (i) The oscillations are the effect of phase difference increase between the eigenstates of the Hamiltonian.
- (ii) The admixture of the eigenstates  $\nu_1, \nu_2$  in a given neutrino state are fixed (by  $\theta$ ).
- (iii) Flavors (flavor composition) of the eigenstates are also fixed (by  $\theta$ ).

### 3.2 Evolution Equation

Let us find the evolution equation which describes a propagation of mixed neutrinos in vacuum [18].

1). For ultra relativistic neutrinos up to corrections of the order  $m_\nu/E$  one can neglect the spin effects and therefore omit the spin structure of the wave functions. Then for a state with definite mass,  $m$ , we can write

$$i\frac{d\nu}{dt} \approx \left(p + \frac{m^2}{2E}\right)\nu. \quad (37)$$

2). For two ultra relativistic states with definite masses  $\nu = (\nu_1, \nu_2)$  the evolution equation is

$$i \frac{d\nu}{dt} \approx \left[ p \cdot I + \frac{(M^{diag})^2}{2E} \right] \nu, \quad (38)$$

where  $(M^{diag})^2 = \text{diag}(m_1^2, m_2^2)$ .

3). Substituting in (38) the expression  $\nu = S^+ \nu_f$ , where

$$\nu_f \equiv \begin{pmatrix} \nu_e \\ \nu_\mu \end{pmatrix}, \quad (39)$$

we get the equation for the flavor states

$$i \frac{d\nu_f}{dt} = \left( p \cdot I + \frac{M^2}{2E} \right) \nu_f. \quad (40)$$

Here

$$M = S(\theta) M^{diag} S(\theta)^\dagger \quad (41)$$

is the mass matrix in flavor basis, and in presence of mixing this matrix is non diagonal.

The first term in the RH side of (40) as well all other contributions proportional to the unit matrix,  $I$ , can be omitted. Finally we get the Schrödinger like equation:

$$i \frac{d\nu_f}{dt} = H_0 \nu_f, \quad H_0 \simeq \frac{M^2}{2E}, \quad (42)$$

where  $H_0$  is the effective Hamiltonian. According to (41), it can be written explicitly in terms of masses and mixing angle as

$$H_0 = \frac{\Delta m^2}{2E} \begin{pmatrix} -\cos 2\theta & \sin 2\theta \\ \sin 2\theta & \cos 2\theta \end{pmatrix}. \quad (43)$$

The solution of equation (42) leads to the standard oscillation formula (34).

### 3.3 Matter effect

At low neutrino energies a medium is transparent for neutrinos. Neutrinos undergo just elastic forward scattering. A state of medium is not changed. In this case the effect of medium is reduced to the appearance of the potential  $V$ :

$$V = \langle \Psi | H_{int} | \Psi \rangle, \quad (44)$$

where  $\Psi$  is the wave function which describes the system of neutrino and medium, and  $H_{int}$  is the Hamiltonian of interaction. According to the standard model there is no flavor changing interactions in the lowest order and the matrix of the potentials in the flavor basis,  $V_f$ , is diagonal:  $V_f = \text{diag}(V_e, V_\mu)$ . Again only difference of the diagonal elements is important and  $V_f$  can be written as  $V_f = \text{diag}(V_e - V_\mu, 0)$ . The difference of the interactions of the electron and muon neutrinos in usual medium is due to scattering of the electron neutrinos on electrons via charged currents. The corresponding Hamiltonian is

$$H_{int} = \frac{G_F}{\sqrt{2}} \bar{\nu} \gamma^\mu (1 - \gamma_5) \nu \bar{e} \gamma_\mu (1 - \gamma_5) e \quad (45)$$

and the explicit calculations for unpolarized medium at rest give  $V_e - V_\mu = \sqrt{2}G_F N_e$ , where  $G_F$  is the Fermi constant and  $N_e$  is the concentration of the electrons.

Total effective Hamiltonian which describes neutrino evolution is  $H = H_0 + V$  with  $H_0$  given in (43). Thus we get the evolution equation for mixed neutrinos in matter:

$$i\frac{d\nu_f}{dt} = H\nu_f, \quad H \simeq \frac{M^2}{2E} + V_f. \quad (46)$$

and

$$V_f = \text{diag}[\sqrt{2}G_F n_e, \quad 0]. \quad (47)$$

### 3.4 Propagation in Matter

In matter the mixing matrix and the eigenstates are determined by the diagonalization condition for the complete Hamiltonian

$$S(\theta_m)^\dagger H S(\theta_m) = H^{diag} \equiv \text{diag}(H_1, \quad H_2). \quad (48)$$

Here  $H_i$ , ( $i = 1, 2$ ) are the eigenvalues of  $H$  and  $S(\theta_m)$  is the mixing matrix in matter which relates neutrino flavor states and the eigenstates in matter  $\nu_H$ :

$$\nu_f = S(\theta_m)\nu_H. \quad (49)$$

Since  $H$  (46) is a function of  $\theta$ ,  $E/\Delta m^2$ , and  $N_e$ , the mixing angle in matter also depends on these parameters. One can find explicitly:

$$\tan 2\theta_m = \frac{\sin 2\theta}{\cos 2\theta - 2\sqrt{2}G_F N_e E/\Delta m^2}. \quad (50)$$

Mixing becomes maximal at the so called the resonance density:

$$N_e^R = \frac{\Delta m^2}{2E} \frac{\cos 2\theta}{\sqrt{2}G_F}. \quad (51)$$

The equation (49) can be “inverted”:

$$\nu_H = S^\dagger(\theta_m)\nu_f. \quad (52)$$

According to (50)  $\theta_m$  determines the *flavor composition* of the neutrino eigenstates. Since  $\theta_m$  depends on  $N_e$ , the flavors of the neutrino eigenstates in matter depend on density too.

Let us find the evolution equation for the eigenstates. Substituting (49) into (46), we get after trivial transformations:

$$i\frac{d\nu_H}{dt} = \left( H^{diag} - iS^\dagger \frac{dS}{dt} \right) \nu_H, \quad (53)$$

where the relation (48) was used. Explicitly the equation (53) can be written as

$$i\frac{d}{dt} \begin{pmatrix} \nu_{1m} \\ \nu_{2m} \end{pmatrix} = \begin{pmatrix} H_1 & i\dot{\theta}_m \\ -i\dot{\theta}_m & H_2 \end{pmatrix} \begin{pmatrix} \nu_{1m} \\ \nu_{2m} \end{pmatrix}. \quad (54)$$

Here  $\dot{\theta}_m \equiv \frac{d\theta_m}{dt}$ .

Let us consider now the neutrino propagation in matter with different density distributions.

*Propagation in matter with constant density* (this corresponds to the propagation of neutrinos inside the Earth: the density profile can be described as several layers with approximately constant densities). In this case:  $N_e = \text{const}$ , so that  $\theta_m = \text{const}$ ,  $\dot{\theta}_m = 0$  and as in the vacuum case the flavors of the eigenstates are fixed. Moreover, the equations for the eigenstates  $\nu_{1m}$  and  $\nu_{2m}$  are splitted, *i.e.* the  $\nu_{1m}$ ,  $\nu_{2m}$  propagate independently. A propagation has a character of oscillations. The only difference is that now the parameters of oscillations (depth, length) are determined by the matter mixing angle  $\theta_m$  and by the difference of the eigenvalues in matter,  $H_2 - H_1$ :

$$A_P = \sin^2 2\theta_m, \quad l_m = \frac{2\pi}{H_2 - H_1}.$$

These values depend on the density and the neutrino energy and differ from the vacuum values.

Note that at certain energy (resonance energy) which depends on density and mass difference, the depth of oscillation becomes maximal and one may have a complete transformation of neutrino flavor, although the vacuum mixing angle can be small. This phenomenon is called the *resonance enhancement of oscillations*.

*Propagation in matter with varying density* (*e.g.*, propagation of neutrinos inside the Sun). The mixing angle  $\theta_m$  changes along the neutrino trajectory, and this change has two crucial consequences: (i). As  $\theta_m$  determines the flavor composition of the neutrino eigenstates according to (52), the change of  $\theta_m$  means the change of flavors of the eigenstates. (ii).  $\dot{\theta}_m$  is non zero; the equations for the eigenstates are not splitted, there are the transitions between the eigenstates:  $\nu_{1m} \leftrightarrow \nu_{2m}$ .

If  $N_e$  changes slowly enough, so that

$$|\dot{\theta}_m| \ll |H_2 - H_1|, \tag{55}$$

then in the first approximation one can neglect  $\dot{\theta}_m$  in the evolution equation (54). The condition (55) is called the *adiabaticity condition*. In the adiabatic approximation the transitions  $\nu_{1m} \leftrightarrow \nu_{2m}$  are neglected, and as in the cases of vacuum and uniform matter the eigenstates propagate independently. In contrast with vacuum and uniform matter cases, now flavor compositions of the eigenstates change according to density change.

For fixed neutrino energy mixing angle depends on density in the following way (see (50)). At small densities:  $\theta_m \approx \theta$ . With increase of density the angle  $\theta_m$  increases and at resonance density,  $N^R$ , equals  $\theta_m = \pi/4$ , so that the mixing becomes maximal. Then  $\theta_m$  increases further and approaches  $\theta_m = \pi/2$  at  $N \gg N^R$ . It is this change of flavor is the origin of flavor conversion. Flavor of neutrino state (averaged over the oscillations) becomes unique function of density, and if the density is changed from  $N \gg N^R$  to  $N \ll N^R$ , the flavor of the state can be changed almost completely.

If the adiabaticity condition is broken in some region, then the transitions  $\nu_{1m} \leftrightarrow \nu_{2m}$  become essential. The probability of transition is determined by the adiabaticity

parameter in the resonance:

$$\kappa_R \equiv \frac{H_2 - H_1}{\dot{\theta}_m} \quad (56)$$

(see eq. (55)). The adiabaticity condition in terms of the adiabaticity parameter is  $\kappa_R \gg 1$ . Using results of general quantum mechanical consideration of the transition between two levels (Landau - Zener formula) one finds:

$$P_{12} = e^{[-\frac{\pi}{2}\kappa_R]}. \quad (57)$$

Adiabaticity violation usually weakens the flavor conversion so that for very strong violation the flavor is not changed.

If  $P_{12} \sim 1$ , there no conversion effect: there is the “double change”: (i) flavor composition is changed completely (ii) there is a complete conversion of the eigenstates:  $\nu_{1m} \rightarrow \nu_{2m}$ . As a result, a flavor state is not changed.

Let us consider the energy dependence of the effect. Suppose neutrinos cross the layer of matter with monotonously decreasing density from some maximal value  $N^{max}$  to zero. (such a situation is realized, *e.g.*, for neutrinos inside the Sun or for neutrinos in the supernovas.)

1). At low energies matter effect can be neglected and the survival probability equals the averaged vacuum oscillations probability.  $P = 1 - 1/2 \sin^2 2\theta$ . With increase of energy the matter effect increases enhancing the transition probability.

2). At energy  $E = E_R(N^{max})$  determined via the resonance condition by maximal density the resonance appears in the layer. And then with increase of energy it shifts to smaller densities. If the adiabaticity condition is fulfilled, then crossing of the resonance will induce strong neutrino transformations. For energies  $E$  for which  $N^R(E) \ll N^{max}$  the initial state coincides practically with the eigenstate  $\nu(0) \equiv \nu_e \approx \nu_{2m}$ , as the result of the adiabatic level crossing final neutrino state (at zero density) will be  $\nu \approx \nu_{2m} = \nu_2$ . The probability to find electron neutrino in this state is evidently

$$P = \sin^2 \theta. \quad (58)$$

3). Explicit expression for the adiabaticity parameter (56) is

$$\kappa_R = \frac{\Delta m^2 \sin^2 2\theta}{2E} \frac{N}{\cos 2\theta \dot{N}}. \quad (59)$$

If  $\dot{N}/N \approx \text{constant}$  (which is true for wide region inside the Sun) then  $\kappa_R \propto 1/E$ , that is with increase of the energy the adiabaticity starts to violate and the survival probability increases. The nonadiabatic edge of the “suppression pit” is described rather reasonably for small mixing angle by Landau-Zener formula (57):  $P \approx P_{12}$ .

Summary:

1). The oscillations are the effect of phase difference increase between the eigenstates of the Hamiltonian. The admixtures of the eigenstates  $\nu_i$  in a given neutrino state are fixed (by  $\theta$ ). Flavors (flavor composition) of the eigenstates are also fixed (by  $\theta$ ).

2). Resonance conversion occurs in medium with monotonously changing density. The resonance conversion is related to change of flavors of the neutrino eigenstates according to density change.

## 4. HINTS

Studies of the solar neutrinos, atmospheric neutrinos, large scale structure of the Universe give the hints to nonzero neutrino masses and lepton mixing. The results from the laboratory experiment LSND may also have an interpretation in terms of neutrino oscillations.

### 4.1 Solar neutrinos

Solar neutrino data give, probably, the strongest hint to non zero masses and mixing (see for review [21]- [23]). Central part ( $R < 0.2R_\odot$ ) of the Sun is the source of the electron neutrinos. Different nuclear reactions produce different components of spectrum: boron-, beryllium-, pp- neutrinos etc.. The spectrum is calculated in the Standard Solar Model (SSM), and the SSM is confirmed by the helioseismology.

According to the SSM main contribution to the energy release comes from the proton-proton cycle and the largest flux is that of pp-neutrinos (the end point of spectrum is 0.42 MeV). The Beryllium neutrino flux (line with energy 0.86 MeV) is the “Next to leading”. And the highest energies are the energies of the boron neutrinos with end point about 14 MeV. (We don’t consider small flux of hep- neutrinos).

Solar neutrinos cross the matter of the Sun, then the space between the Sun and the Earth and then the matter of the Earth (appreciable amount during the night) and finally are detected by underground installations. At present five installations measure signals of the solar neutrinos.

- Homestake experiment (based on the reaction  $\nu_e + {}^{37}\text{Cl} \rightarrow {}^{37}\text{Ar} + e$ ) has energy threshold of the reaction  $E_{th} = 0.81$  MeV;
- Kamiokande experiment (detection of the recoil electrons from  $\nu + e \rightarrow \nu + e$ ) has the experimental threshold  $E = 7.5$  MeV.
- Superkamiokande (super version of Kamiokande) will have threshold about 5 MeV.
- Two gallium experiments, the SAGE and GALLEX with basic reaction  ${}^{71}\text{Ga} + \nu_e \rightarrow {}^{71}\text{Ge} + e$  are sensitive to neutrinos with  $E > E_{th} = 0.233$  MeV.

The detectors have different thresholds and therefore are sensitive to different parts of the neutrino spectrum. Therefore already with existing data one can perform *the spectroscopy of solar neutrinos*.

Let us summarize main results. The ratios of signals observed by the Chlorine [24],  $\nu e$  scattering [25] and Gallium [26], [27] experiments to those predicted by the SSM [22],  $R \equiv (\text{observed})/(\text{predicted})$ , are respectively:

$$R_{Ar} \sim 0.27 \pm 0.04, \quad R_{\nu e} \sim 0.42 \pm 0.08 \quad R_{Ge} \sim 0.53 \pm 0.08 . \quad (60)$$

Kamiokande does not see the effects of distortion of the boron neutrino spectrum. This real time experiment does not see also time variations of signals: day/night, seasonal correlated to the solar activity. Best description of the GALLEX data corresponds to practically constant neutrino flux.

Immediate observation from (60) is that

- All experiments have registered a deficit of the neutrino flux. The exception could be the Kamiokande /Superkamiokande result which could be consistent with low flux models predictions.

- The deficit is different in different experiments. The suppression in K/SK and Gallium experiments  $R_{Ge} \approx R_{\nu e} \sim 0.5$ , the Homestake signal is suppressed stronger.

Deeper insight into the problem follows from two observation:

- (i) The Ar-production rate by boron neutrino flux, as measured by Kamiokande and SK, is bigger than total Homestake signal:

$$Q_{Ar}^B > Q_{Ar}^{Hom} \quad (61)$$

- (ii) The observed Ge- production rate is at the level of Ge-production rate by pp-neutrino flux which follow from solar luminosity:

$$Q_{Ge}^{exp} < Q_{Ge}^{pp} . \quad (62)$$

Both facts testify for a strong suppression of the Beryllium neutrino flux. This suppression can not be explained just by variations of solar models.

Real understanding of the problem follows from solar neutrino spectroscopy which does not refer to any specific solar model [28] - [45].

Fluxes of the electron neutrinos in the Earth detectors,  $F_i(E)$ , ( $i = pp, Be, pep, N, O, B$ ), can be written as

$$F_i(E) = P(E) \cdot f_i \cdot F_i^0(E) , \quad (63)$$

where  $F_i^0$  are the fluxes in the reference standard solar model (RSSM).

Factors  $P(E)$  are the electron neutrino survival probabilities:  $\nu_e \rightarrow \nu_e$ . They describe possible effects of neutrino transformations and can be called the *neutrino factors*. These factors depend on neutrino parameters:  $\Delta m^2, \theta, E$  as well as on characteristics of the Sun – density, magnetic fields *etc.*, and satisfy the restriction  $0 \leq P(E, \theta, \Delta m^2) \leq 1$ .

On the contrary,  $f_i$  are the *solar model factors* which describe deviation of true original neutrino fluxes from those predicted by the reference SSM. The product  $f_i \cdot F_i^0$  is the original flux of  $i$ -component, so that  $f_i$  can be considered as the flux in the units of the reference model flux.

*The problem* is to find separately  $f_i$  and  $P(E)$  from the solar neutrino data. If the Sun is “standard”, then  $f_i = 1$ . For “standard” neutrinos (massless, unmixed) we take  $P = 1$ .

Main results of the spectroscopy can be summarized in the following way [45]:

K/SK give immediately an information about energy spectrum of the boron neutrinos. Due to strong smoothing in the recoil electron spectrum, even strong distortion of the neutrino spectrum leads to approximately linear energy dependence of the ratio of the observed and the detected events (recoil electrons with a given energy):

$$R_e(E) \approx R_e(E_0) \left[ 1 + s_e \cdot \frac{(E - E_0)}{E_0} \right] . \quad (64)$$

$R_e \equiv N^{obs}/N^{th}$ . Thus, a distortion can be characterized by the *slope parameter*,  $s_e$ , which equals  $s_e \equiv [(dR_e/dE)/E_0 R_e]_{E_0}$ . We fix the slope in the middle of the detected interval at  $E_0 = 10$  MeV - for definiteness. The  $\chi^2$  fit of Kamiokande spectrum by (64) gives

$$s_e = 0.4 \pm 0.5 , \quad (1\sigma) . \quad (65)$$



The best fit point corresponds to  $\chi^2 = 9$  for 6 d.o.f.. Although the best fit corresponds to non zero slope, the data agree well with an absence of any distortion. In the same time the data do not exclude rather strong distortion.

The analysis of data can be performed in three steps.

1. Using Kamiokande/SK data one fixes to the boron neutrino flux ( $f_B P_B$ ).
2. Subtracting from Homestake signal the effect of boron neutrinos as measured by K/SK, one gets information about fluxes of the intermediate energies (first of all about  ${}^7\text{Be}$  neutrinos).
3. Subtracting from Gallium data, the effects of high energy and intermediate energy neutrinos as measured by Homestake and K/SK one finds the pp-neutrino flux. Such an analysis leads to suppression profiles shown in fig. 2 - 5. The profiles depend on whether other neutrinos apart from electron neutrino are present in the solar flux or not (for more detail see [45]).

In the case of zero (small) non electron neutrino flux (fig. 2) typical suppression profile has moderate suppression at high energies  $E > 7.5$  MeV, strong suppression at the intermediate energies and weak (or absence of) suppression at low energies.

If one admits an existence of the “non electron” neutrino fluxes, the spectroscopy can lead to quite different picture of suppression (fig. 3 - 5). In particular, the Beryllium neutrino flux may not be suppressed for sufficiently large contribution of non- electron neutrinos to K/SK signal.

These results should be confronted with predictions from different solutions of the problem.

The *astrophysical solutions* – most of them are based on diminishing of the central temperature of the Sun. The astrophysical solution gives typical suppression profile with intermediate energies being suppressed weaker then the high energies. There is no non-electron neutrinos in this case, so that the profile should be compared with that in fig.2. Obvious difference between profiles is a basis of the conclusion that the astrophysical solutions are very strongly disfavored.

There are some attempt to diminish flux of the  ${}^7\text{Be}$ -neutrinos. However the helioseismological data leave smaller and smaller room for changes of the conditions (even in the center of the Sun) which lead to appreciable changes of neutrino fluxes. Any suggested modifications of physical conditions which do not contradict helioseismological data give too small changes of the neutrino fluxes.

Still one should remember that interpretation of some experimental results may be incorrect. In fact, some experimental features are not explained and may not be just statistical effect.

Let us consider solutions based on assumption of non zero masses and mixing.

*Vacuum oscillations solution.*

The oscillations of neutrinos between the Sun and the Earth with oscillation length comparable with distance between the Sun and the Earth [46] (for recent analysis see [47]

- [50]) may give reasonable approximation to the desired profiles of fig. 4, 5 even for SSM.

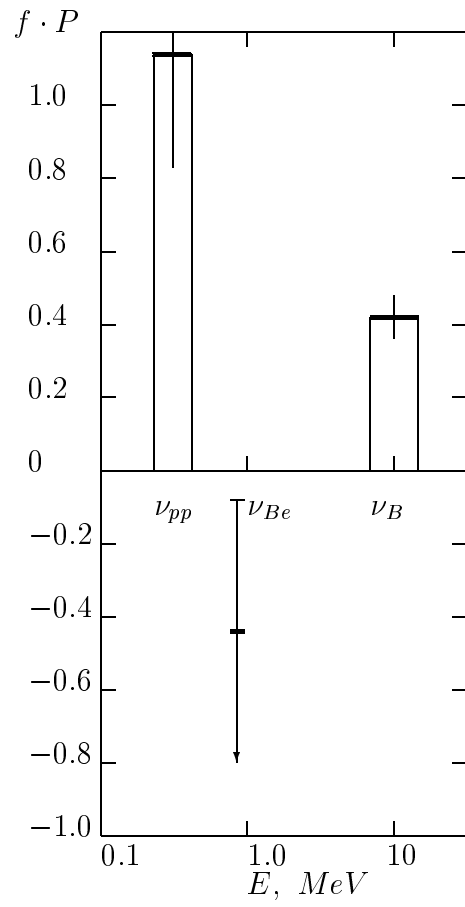


Fig. 2. Solar neutrino spectroscopy. The dependence of suppression factor on neutrino energy. There is no muon or tau neutrinos in the solar neutrino flux.

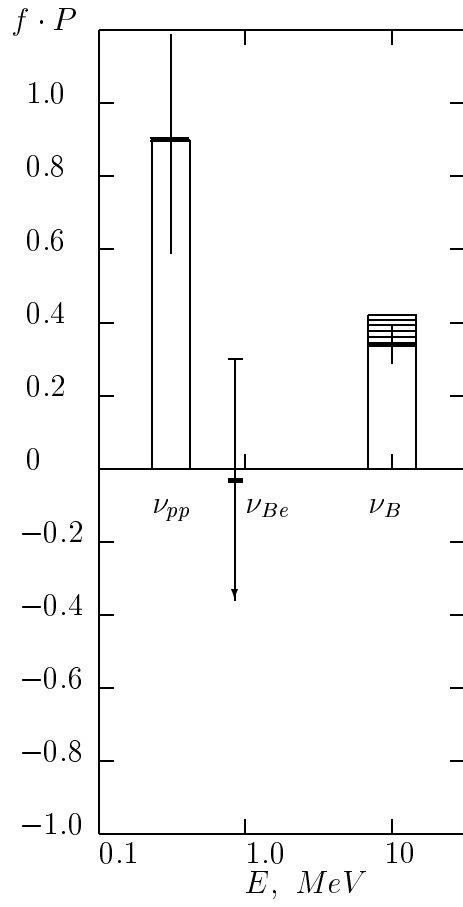


Fig. 3. Solar neutrino spectroscopy. The dependence of suppression factor on neutrino energy. The effective probability of transition to the muon (tau) neutrino in the boron neutrino range  $\langle P_B \rangle = 0.6$  Shaded region is the contribution of muon (tau) neutrino flux to the Kamiokande/SK signal.

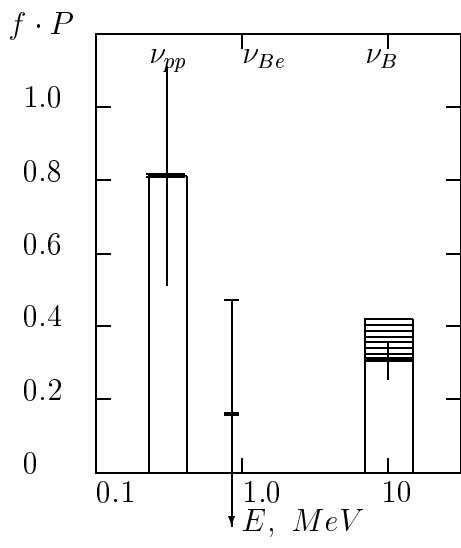


Fig. 4. The same as in fig. 3 for  $\langle P_B \rangle = 0.3$

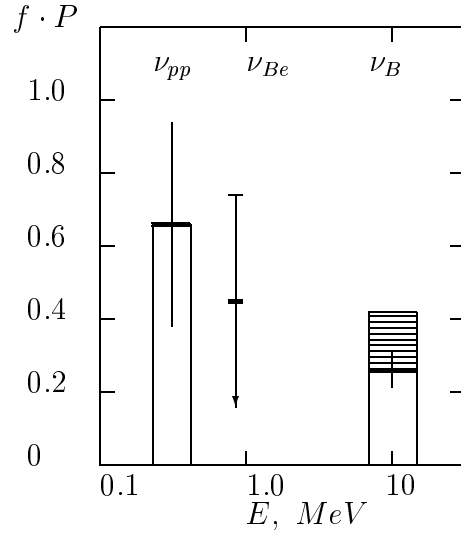


Fig. 5. The same as in fig. 3 for  $\langle P_B \rangle = 0.2$

Main region of the oscillation parameters ( $\Delta m^2 \sim 3 \cdot 10^{-11} - 10^{10} \text{ eV}^2$ ) corresponds to half oscillation length

$$\frac{1}{2}l_\nu(E_B \sim 10\text{MeV}) \gtrsim R_E, \quad (66)$$

where  $E_B \sim 10 \text{ MeV}$  is the typical energy of the high energy part of the boron neutrino spectrum,  $R_E$  is the radius of Earth orbit. From the condition (66) we get  $\Delta m^2 < 10^{10} \text{ eV}^2$ . For small values of  $f_B$  also a region of very small  $\Delta m^2 \sim 5 \cdot 10^{-12} \text{ eV}^2$  is allowed [48].

Mixing angle should be large. The bound follows from the Kamiokande/Homestake data: For RSSM one gets  $\sin^2 2\theta > 0.7$ . However, such a large mixing is disfavored by the data from SN1987A [51]. For large mixing the transitions  $\bar{\nu}_\mu \leftrightarrow \bar{\nu}_e$  ( $\bar{\nu}_\tau$ ) result in modification of the  $\bar{\nu}_e$ -energy spectrum. In particular, the appearance of high energy tail is expected, since the original  $\bar{\nu}_\mu$  ( $\bar{\nu}_\tau$ ) energy spectrum has a larger average energy than the spectrum of  $\bar{\nu}_e$ . The events with  $E > 40 - 50 \text{ MeV}$  are predicted in contrast with observations. The excluded region covers the region of “just-so” solution.

Depending on neutrino parameters and  $f_B, f_{Be} \dots$  one can get variety of distortions of the boron neutrino energy spectrum [48].

*Resonance flavor conversion.*

*Small mixing solution.* The dependence of the suppression factor on energy [52] perfectly fits the configuration (Fig. 3,4). The best fit point corresponds to  $\chi^2 \approx 0.3 - 0.4$  for 2 d.o.f.. Note that additional contribution to Kamiokande  $\Delta f_B \approx 0.09$ , follows from scattering of the converted  $\nu_\mu$  ( $\nu_\tau$ ) on electrons due to the neutral currents.

A consistent description of the data has been found for [40]

$$f_B \sim 0.4 - 2.0.$$

The mass squared difference

$$\Delta m^2 = (6 \pm \frac{4}{3}) \cdot 10^{-6} \text{ eV}^2 \quad (67)$$

is restricted essentially by Gallium results.

For  $f_B \sim 0.5$ , and  $\sin^2 2\theta \sim 10^{-3}$ , all effects of conversion in the high energy part of the boron neutrino spectrum ( $E > 5 - 6 \text{ MeV}$ ) become very weak. In particular, a distortion of the energy spectrum disappears, and ratio charged-to-neutral currents  $(CC/NC)^{exp}/(CC/NC)^{th}$  approaches 1. Thus studying just this part of spectrum it will be difficult to identify the solution (e.g., to distinguish the conversion and the astrophysical effects).

*Large mixing MSW* solution also gives reasonable fit of the data. Typical energy dependence fits well the configuration shown in fig. 5. Relevant neutrino parameters range is

$$\Delta m^2 = (6 \cdot 10^{-6} - 10^{-4}) \text{ eV}^2, \quad \sin^2 2\theta = 0.65 - 0.85. \quad (68)$$

The problem can be solved also by the *conversion into sterile neutrino* (the state which has no usual weak interactions):  $\nu_e \rightarrow S$ .

The regions of neutrino parameters are approximately the same as in flavor case if one restricts the original boron neutrino flux by  $f_B \leq 2$ .

The analysis of data in terms of two neutrino mixing is quite realistic, since in the most interesting cases (simultaneous solution of the solar and hot dark matter problems, or solar and atmospheric neutrino problems) third neutrino has large mass so that its  $\Delta m^2$  is beyond the resonance region and its mixing to the electron neutrino is rather small. This reduces the three neutrino task to the case of two neutrino mixing. However, there is one interesting example where third neutrino could influence the solutions of the solar neutrino problem. It was considered previously [53, 54, 55] and reanalyzed recently in [56, 57]: The third neutrino is in the region of the solution of the atmospheric neutrino problem (see sect. 7.4):  $m_3 \sim 0.1$  eV and it has an appreciable admixture to the electron neutrino state.

In this case additional regions of the neutrino parameters  $\Delta m^2 = (10^{-5} - 10^{-6})$  eV<sup>2</sup> and  $\sin^2 2\theta = 3 \cdot 10^{-4} - 3 \cdot 10^{-3}$  are allowed for  $\cos^4 \phi \sim 0.5 - 0.7$ .

## 4.2 Atmospheric Neutrinos

Atmospheric neutrinos (see reviews [58], [59]) are produced mainly by the decays of pions and muons which in turn appear in interactions of cosmic rays with nuclei of atmosphere. Depending on energies, these neutrinos induce events of different types in the underground installations. In particular, at sufficiently low energies ( $E < 10$  GeV) neutrino interactions (leading to the production of muons and electrons) manifest itself as contained (inside the detectors) or partially contained muon-like and the electron-like events.

The atmospheric neutrino problem is the deficit of the muon-like events in comparison with the electron-like events. The ratio  $(\mu - like)/(e - like)$  is predicted (Monte-Carlo simulations) with rather good accuracy: uncertainties are estimated to be less than 5%. The observed ratio (Kamiokande, IMB) is about 60% of the expected one, so that the double ratio equals:

$$R_{\mu/e} \equiv \frac{(\mu - like)/(e - like)_{data}}{(\mu - like)/(e - like)_{MC}} = 0.55 - 0.65. \quad (69)$$

This deficit can be explained by oscillations of the muon neutrinos into electron, or tau or sterile neutrino. The relevant region of neutrino parameters is

$$\Delta m^2 = 10^{-3} - 10^{-1} \text{ eV}^2, \quad \sin^2 2\theta > 0.5. \quad (70)$$

Main question is whether the result is really due to the oscillations or due to some methodics, backgrounds etc.. Let us summarize the important points of discussion.

- *Frejus negative result.* The Frejus detector has not found the anomaly:  $R_{\mu/e} = 0.87 \pm 0.21$ . Although the error bars are large and positive results are just two sigma below. NUSEX collaboration has given 1 for the double ratio but positive signal is only 1 sigma below.
- *Upward going muons.* No deficit of muon neutrinos has been found in the detection of the high energy muon neutrinos. Observed numbers of the so called upward going muons produced by these neutrinos in the rock surrounding detectors (Baksan, Kamiokande) are in agreement with expected numbers. The expected numbers, however, are determined by the absolute value of the flux. And the absolute value has quite large (up to 30 - 40 %) uncertainties. But even for conservative values of fluxes the bounds exclude practically all parameter region (70).

However, it should be noted that preliminary results from MACRO detector (Gran-Sasso) show some (about  $2\sigma$ ) deficit of the flux.

- *Stopping-to-through going muons.* With certain probability muons produced by neutrinos stop in the detector and decay (“stopping muons”). Typical energy of neutrinos responsible for these muons (2 - 20 GeV) is lower than the average energy of neutrinos generating through-going muons which just cross the detectors ( $10 - 10^3$  GeV). Due to this energy dependence, the ratio of stopping to through going muons is sensitive to oscillations. On the other hand the ratio does not depend on the absolute values of the fluxes which makes the results more reliable. The IMB collaboration has not found a deviation of the measured ratio from calculated one. This allows one to exclude some region of the positive results (70).

The conclusion, however, depends on the neutrino cross-sections and on the energy spectrum. It is argued that the latter is not well known at large energies, to make firm conclusion.

- *Multi-GeV events: angular dependence.* Analyzing the contained and partially contained events with energies above 1.3 GeV the Kamiokande collaboration [60] has found a dependence of the double ratio  $R_{\mu/e}$  on the zenith angle  $\theta_Z$ . The ratio increases with  $\cos \theta_Z$ . The dependence can be explained by oscillations with almost maximal mixing and oscillation length about 300 - 1000 km. At low energies (sub-GeV events) the angular dependence disappears because the oscillation length is small and the oscillations are averaged out for all angles. Being confirmed the  $\theta_Z$ -dependence will be the proof of the oscillation interpretation. However, at the moment the statement about existence of the angular dependence is not compelling. It is based essentially on the excess of the  $\mu$  like events in one angular bin in which the muon arrive from the above. There is also an appreciable excess of the e-like events in the direction from the center of the Earth. For the oscillation length under discussion, however, one does not expect the observed strong dependence for upward going electrons.
- *No misidentification.* The calibration experiment at KEK has shown that e-like and  $\mu$ -like events are identified in water Cherenkov detector correctly: There is no room to explain the effect by the misidentification.
- *Methodics and SOUDAN result.* The deficit has been observed in the water Cherenkov detectors in the same time no deficit has been found in the iron track calorimeters (Frejus, Nusex). (Although the error bars in these experiments are large and they are only  $2\sigma$  above the Kamiokande/IMB result.) Does this mean that the origin of the deficit is the methodics of the experiment? In this connection the SOUDAN experiment result (calorimeter experiment with larger volume improved methodics and larger statistics) is very important. The latest results [61]:

$$R_{\mu/e} \equiv 0.72 \pm 0.19^{+0.05}_{-0.07} \quad (71)$$

still can not be considered as decisive.

- *Dependence on the depth?* The tendency was marked that the deeper the installation the weaker “anomaly”. The smallest “ $R_{\mu/e}$ ” is from IMB detector (the depth 1800 m.v.e. -meters of water equivalent) and there is no anomaly in Frejus (4500 m.v.e.). The deeper the installation the smaller background [62]. Conclusion: atmospheric anomaly is the background effect?

- *Neutron background.* Neutrons are produced in interactions of muons with nuclei in the rock surrounding the installations. Neutrons diffuse inside the detector and interacting with nuclei produce (in particular) neutral pions. Two gamma quanta from pion decay generate the EM shower which imitate the e-like event. It is claimed [62] that this can solve the problem. Clearly, neutron events should be concentrated near the walls of the detectors. Kamiokande collaboration argues that the effect is negligibly small. Recent studies of the vertex distributions in the detector have given that the neutron contamination the sub-GeV e-like sample is smaller than 1.2% (90% C.L.) [63].  
Also the neutron signal has not been observed by SOUDAN experiment.
- *Double ratio or two ratios? Consistency.* Some information can be hidden in the double ratio. It was pointed out [64] that although there is an agreement in  $R_{\mu/e}$  two separate ratios  $\mu/\mu_{MC}$  and  $e/e_{MC}$  are different, *e.g.*, for the sub- and multi-GeV events in Kamiokande. Moreover the disagreement can not be removed completely by oscillations.
- *Reactors bound.* No oscillations  $\bar{\nu}_e \rightarrow \text{anything}$  has been observed in the reactor experiments BUGEY-3 [65] and Krasnoyarsk [66]. The excluded region of the neutrino parameters covers practically all region of solutions (sub + multi GeV data) in the case of  $\nu_\mu - \nu_e$  oscillations.

Let us compare situations with atmospheric and solar neutrinos. In the case of solar neutrinos there are solutions which give excellent fit of data. Moreover there are several solutions which give a good fit. As far as concerning the atmospheric neutrinos, the oscillations seem to be the only viable explanation, but even this explanation does not give good description of all data.

The problem can be resolved by SuperKamiokande, CHOOZ and forthcoming long base line accelerator experiments.

### 4.3 Neutrino mass and the peculiar velocities of pulsars

There is the long standing problem of explanation of the high peculiar velocities of pulsars ( $v \sim 500$  km/s). Non-symmetric collapse, effects in binary systems *etc.*, give typically smaller velocities. It looks quite reasonable to relate these velocities with neutrino burst [67]. The momenta of pulsars are  $10^{-3} - 10^{-2}$  of the integral momentum carried out by neutrinos. Therefore,  $10^{-3} - 10^{-2}$  asymmetry (anisotropy) in neutrino emission is enough to solve the problem [67].

The anisotropy of neutrino properties can be related to the magnetic field. It was suggested that very strong magnetic field ( $10^{15} - 10^{16}$  Gauss) can influence weak processes immediately: the probabilities of emission of neutrinos along the field and against the field are different.

According to mechanism suggested in [68] the magnetic field influences the resonance flavor conversion of neutrinos thus leading to angular asymmetry of the conversion with respect to the magnetic field. The latter results in asymmetry of the neutrino properties.

Let us give some details. Polarization of medium modifies the potentials. Instead of (47), we get

$$V = \sqrt{2}G_F n_e \left[ g_V + g_A 2(\vec{k} \cdot \langle \vec{s} \rangle) \right] , \quad (72)$$



where  $\vec{k} \equiv \vec{p}/p$ , and  $\vec{p}$  is the momentum of neutrino,  $\langle \vec{s} \rangle$  is the averaged vector of spin of electrons in medium. Electrons are polarized by the magnetic field. The polarization is determined by concentration of electrons in the lowest Landau level. For strongly degenerate gas and in the limit of small field one finds:

$$2\langle \vec{s} \rangle = -\frac{n_0}{n_e} = -\frac{e\vec{B}}{2n_e} \left( \frac{3n_e}{\pi^4} \right)^{1/3}. \quad (73)$$

This leads to the result

$$V = \sqrt{2}G_F n_e \left[ 1 - \frac{e(\vec{k} \cdot \vec{B})}{2n_e} \left( \frac{3n_e}{\pi^4} \right)^{1/3} \right], \quad (74)$$

It is assumed that the resonance layer for the conversion  $\nu_e \rightarrow \nu_\tau$  lies between the  $\nu_e$ -neutrinosphere and  $\nu_\tau$ -neutrinosphere (the latter is deeper than the former due to weaker interactions of  $\nu_\tau$ ). Thus the  $\nu_\tau$  which appear in the resonance layer will propagate freely and  $\nu_e$ 's are immediately absorbed. The resonance layer becomes the “neutrinosphere” for  $\nu_\tau$ . (In fact, in presence of the magnetic field the neutrinosphere becomes “neutrinoellipsoid” and this is crucial for the mechanism).

It is assumed that inside the protoneutron star there is a strong magnetic field of the dipole type. Then in one hemisphere the field is directed outside the star, so that for neutrinos leaving the star  $(\vec{k} \cdot \vec{B}) > 0$ , whereas in another hemisphere the field points towards the center of star and  $(\vec{k} \cdot \vec{B}) < 0$ . The magnetic field modifies the resonance condition differently in these two hemispheres. In hemisphere with  $(\vec{k} \cdot \vec{B}) > 0$ , the resonance condition is satisfied at larger densities and larger temperatures;  $\nu_\tau$  emitted from this hemisphere will have bigger energies. In opposite hemisphere with  $(\vec{k} \cdot \vec{B}) < 0$  the resonance is at lower densities and lower temperatures and neutrinos have smaller energies. Thus presence of the magnetic field leads to difference in energies of  $\nu_\tau$  emitted in different directions and therefore neutrino burst knocks the star. The observed velocities imply the polarization effect  $10^{-3} - 10^{-2}$ , or according to (74)

$$\frac{eB}{n_e} \left( \frac{3n_e}{\pi^4} \right)^{\frac{1}{3}} \sim 10^{-3} - 10^{-2}.$$

In the  $\nu_e$ -neutrinosphere:  $n_e \sim 10^{11} \text{ cm}^{-3}$  which gives  $B \sim 10^{13} \text{ Gauss}$ . From the condition that the resonance should be below the  $\nu_e$ -neutrinosphere one gets

$$\Delta m^2 > 10^4 \text{ eV}^2, \text{ or } m_3 > 100 \text{ eV}. \quad (75)$$

The mixing angle can be rather small: from the adiabatic condition it follows that  $\sin^2 2\theta > 10^{-8}$ .

Thus explanation of the peculiar velocities of pulsars based on the resonance flavor conversion implies the mass of the heaviest ( $\sim \nu_\tau$ ) neutrino bigger than 100 eV. To avoid the cosmological bound on mass, the neutrino must decay (e.g. with Majoron emission).

In connection with Kusenko-Segre proposal [68] it is interesting to recall recent tritium experiment results [6] which may be explained by admixture of the 200 eV neutrino in  $\nu_e$ .

#### 4.4 Hot Dark Matter

There is a number of studies of the structure formation for value of the Hubble constant  $h = 0.5$  and  $\Omega = 1$  [69]. A good fit of the data can be obtained in the so called mixed scenario with dominating contribution of the cold dark matter  $\Omega = 0.7 - 0.8$  and the rest contribution  $\Omega_{HDM} \sim 0.2$  from the hot dark matter [70], [71] [72]. The natural candidate for the hot dark matter is the relic neutrinos with mass 5 - 7 eV. Even better fit can be achieved for two types of neutrinos with masses 2 - 3 eV, so that total  $\Omega_{HDM}$  is the same but the epoch when this neutrinos become nonrelativistic is later and scale  $1/m_\nu$  is bigger.

It should be noted that scenario with HDM is not the only possibility. Good fit can be achieved by, e.g., modification of the spectrum of original density perturbations (deviation from Zeldovich - Harrison spectrum). Also the possibilities with nonzero cosmological constant exist.

Independently on whether neutrinos as HDM exist or not, the Large scale structure formation of the Universe can be used to put upper bound on the neutrino mass. Indeed, pure hot dark matter scenario (light neutrinos) certainly does not explain the structure. Dominating component should be the cold one [70], [71] [72]. Good fit of the cosmological data can be obtained if the hot component contributes less than 30%. For  $\Omega_\nu < 0.3$  one finds the “structure formation bound”:

$$\sum_i m_i < 15 \text{ eV}. \quad (76)$$

#### 4.5 LSND

KARMEN [73] and LSND [74] collaborations are looking for the oscillations of neutrinos from pion decay:  $\pi^+ \rightarrow \mu^+ \nu_\mu$ ,  $\mu^+ \rightarrow e^+ \bar{\nu}_\mu \nu_e$ . The best sensitivity is for the mode  $\bar{\nu}_\mu - \bar{\nu}_e$ , where the background from the primary beam is rather small and there is a good experimental signature:  $\bar{\nu}_e$  interacts as  $\bar{\nu}_e + p \rightarrow n + e^+$  and both products of the reaction – neutron and positron – are detected. The correlation of signals from the positron and neutron is the main criteria for selection. No signal of the neutrino oscillations has been found by KARMEN. At certain experimental cut off conditions 22 events have been observed by LSND in the energy interval 36 - 60 MeV, whereas  $4.6 \pm 0.6$  are expected from known sources.

The observed excess does not exclude the interpretation in terms of neutrino oscillations with probability

$$P_{tr} = (0.31 \text{ }^{+0.11}_{-0.10} \pm 0.05) \text{ } \%$$

In the range of small masses:  $\Delta m^2 < 3 \text{ eV}^2$  the allowed region can be approximated by

$$\Delta m^2 (\text{eV}^2) \sim \frac{6 \cdot 10^{-2}}{(\sin^2 2\theta)^{1/2}}, \quad \sin^2 2\theta \sim 1.5 \cdot 10^{-3} - 4 \cdot 10^{-2}. \quad (77)$$

There is a number of questions concerning LSND result [75] and one needs more data to make any conclusion. In any case it is interesting to look at the region of parameters (77) which may be related to both the cosmological neutrino masses and atmospheric neutrino problem.

## 5. IMPLICATIONS

### 5.1 Neutrino anomalies

Existing neutrino anomalies imply strongly different scales of  $\Delta m^2$ . For the solar neutrinos, atmospheric neutrinos and LSND we have correspondingly:

$$\Delta m_{\odot}^2 \sim (0.3 - 1.2) \cdot 10^{-5} \text{ eV}^2, \quad (78)$$

$$\Delta m_{atm}^2 \sim (0.3 - 3) \cdot 10^{-2} \text{ eV}^2, \quad (79)$$

$$\Delta m_{LSND}^2 \sim (0.2 - 2) \text{ eV}^2. \quad (80)$$

That is

$$\Delta m_{LSND}^2 \gg \Delta m_{atm}^2 \gg \Delta m_{\odot}^2. \quad (81)$$

The mass scale which gives the HDM component of the Universe,  $m_{HDM}$ :

$$m_{HDM}^2 \sim (1 - 50) \text{ eV}^2 \quad (82)$$

can cover the LSND range.

In the case of three neutrinos there is an obvious relation:

$$\Delta m_{21}^2 + \Delta m_{32}^2 = \Delta m_{31}^2, \quad (83)$$

and inequality (81) can not be satisfied. That is, with three neutrinos it is impossible to reconcile all the anomalies. Furthermore, additional larger scale is needed for explanation of pulsar velocities (75).

Three different possibilities are discussed in this connection. One can

- suggest (stretching the data) that

$$\Delta m_{LSND}^2 = \Delta m_{atm}^2; \quad (84)$$

Also the possibility  $\Delta m_{\odot}^2 = \Delta m_{atm}^2$  was discussed.

- “sacrifice” at least one anomaly, *e.g.* the LSND result, or atmospheric neutrinos;
- introduce additional neutrino states.

In what follows we will consider the most appealing possibilities.

Note that typically  $m_{HDM} > m_{ee}$ , where  $m_{ee}$  is the effective mass of the electron neutrino.

### 5.2 “Standard” scenario

The mass spectrum and mixing pattern are shown in fig. 6.

- Second mass,  $m_2$ , is in the range

$$m_2 = (2 - 3) \cdot 10^{-3} \text{ eV}, \quad (85)$$

so that the resonance flavor conversion  $\nu_e \rightarrow \nu_\mu$  solves the solar neutrino problem. The desired mixing angle is consistent with expression

$$\theta_{e\mu} = \sqrt{\frac{m_e}{m_\mu}} - e^{i\phi} \theta_\nu, \quad (86)$$

where  $m_e$  and  $m_\mu$  are the masses of the electron and muon,  $\phi$  is a phase and  $\theta_\nu$  is the angle which comes from diagonalization of the neutrino mass matrix. The relation between the angles and the masses (86) is similar to the relation in quark sector and follows naturally from the Fritzsch ansatz for mass matrices. Such a possibility can be realized in terms of the see-saw mechanism of mass generation.

- The third neutrino has the mass about 5 eV and composes the desired hot component of the dark matter.
- Neutrino masses are generated by the see-saw mechanism. For  $m_2^D = m_c$  at GU scale where  $m_c$  is the mass of charm quark the light mass (85) leads via the see-saw formula to the Majorana mass of the RH neutrino:

$$M_2 \sim (2 - 4) \cdot 10^{10} \text{ GeV} . \quad (87)$$

(Here the renormalization of mass relation in the Minimal supersymmetric standard model has been taken into account). For  $m_3^D \sim m_t$  the mass of  $\nu_3$  leads via the see-saw mechanism to the Majorana mass of the RH neutrino

$$M_3 \sim (4 - 8) \cdot 10^{12} \text{ GeV} . \quad (88)$$

Thus both solar neutrinos and HDM testify for an existence of the intermediate mass scale:  $M_I \sim 10^{13} \text{ GeV}$  so that  $m_W \ll M_I \ll M_P$ .

Note that the values of masses are in agreement with “linear” hierarchy:  $M_2/M_3 \approx m_c/m_t$  [76].

- The decays of the RH neutrinos with mass  $10^{10} - 10^{12} \text{ GeV}$  can produce the lepton asymmetry of the Universe which can be transformed by sphalerons in to the baryon asymmetry [77].
- Simplest schemes with quark - lepton symmetry lead to mixing angle for the  $e-$  and  $\tau-$  generations:  $\theta_{e\tau} \sim (0.3 - 3)V_{td}$ . This value is close to the bound from the nucleosynthesis of heavy elements (r-processes) in the inner parts of the supernovas:  $\sin^2 2\theta_{e\tau} < 10^{-5}$  ( $m_3 > 2 \text{ eV}$ ) [78].

(vi) For  $\mu-\tau$  mixing one expects [79]  $\theta_{\mu\tau} \sim kV_{cb}\eta$ , where  $k = 1/3-3$  and  $\eta \sim 0.6-0.7$  is the renormalization factor. If  $m_3 > 3 \text{ eV}$  some part of expected region of mixing angles is already excluded by FNAL 531. A large part of the region can be studied by CHORUS and NOMAD. The rest (especially  $m_3 < 2 \text{ eV}$ ) could be covered by E803.

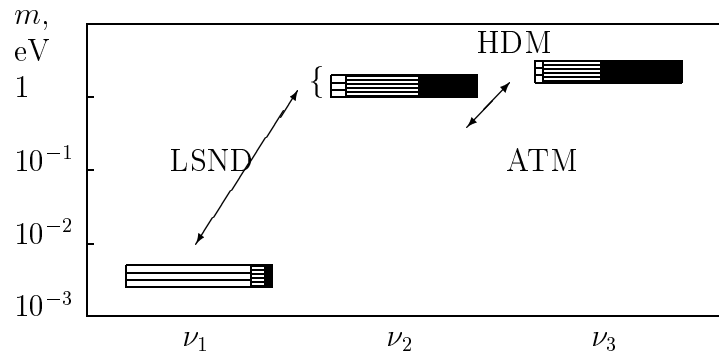


Fig. 6. Qualitative pattern of neutrino masses and mixing. Boxes correspond to different mass eigenstates. The sizes of different regions in the boxes determine flavors ( $|U_{if}|$ ) of given eigenstates. Weakly hatched regions correspond to the electron flavor, strongly hatched regions depict the muon flavor and black regions present the tau flavor. Arrow connects the eigenstates involved in the conversion which solves the solar neutrino problem. “Standard scenario”.

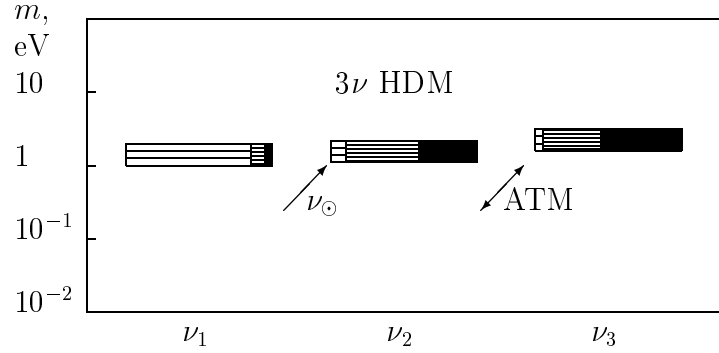


Fig. 7. The same as in fig. 6 for scenario with strongly degenerate neutrino spectrum. Arrow “ATM” connects the eigenstates involved in the oscillations which solves the atmospheric neutrino problem.

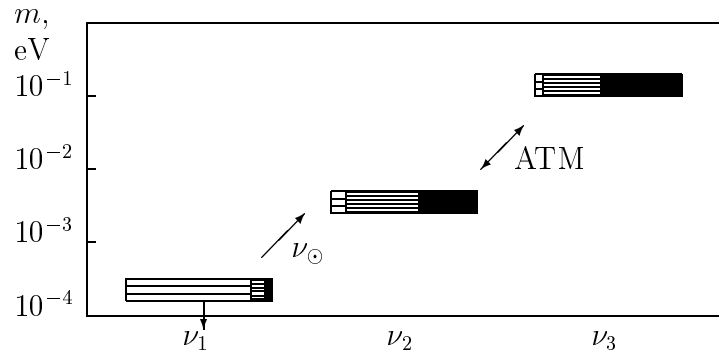


Fig. 8. The same as in fig. 6 for scenario Solar + Atmospheric neutrinos.

- The depth of  $\bar{\nu}_\mu - \bar{\nu}_e$  oscillations with  $\Delta m^2 \approx m_3^2$  equals  $4|U_{3\mu}|^2|U_{3e}|^2 \approx 4|\theta_{e\tau}|^2|\theta_{\mu\tau}|^2$ . The existing experimental bounds on  $\theta_{e\tau}$  and  $\theta_{\mu\tau}$  give the upper bound on this depth:  $< 10^{-3}$  [80] which is too small to explain the LSND result.

### 5.3 Degenerate neutrinos

The standard scenario does not solve the atmospheric neutrino problem. Solar, atmospheric and HDM problem can be solved simultaneously, if neutrinos have strongly degenerate mass spectrum  $m_1 \approx m_2 \approx m_3 \sim 1 - 2$  eV [81, 82, 55], with  $\Delta m_{12}^2 = \Delta m_\odot^2 = 6 \cdot 10^{-6}$  eV<sup>2</sup> and  $\Delta m_{23}^2 = \Delta m_{atm}^2 = 10^{-2}$  eV<sup>2</sup> (fig.7).

The corresponding mass matrix may have the form [82]

$$m = m_0 I + \delta m, \quad (89)$$

where  $I$  is the unit matrix,  $\delta m \ll m_0 \approx 1 - 2$  eV. Moreover (89) can be realized in unique see-saw mechanism with non zero direct Majorana masses of the left components. Main contribution,  $m_0$ , originates from interaction with Higgs triplets which respects some horizontal symmetry like  $SU(2)$ ,  $S_4$  or permutation symmetry. It looks quite interesting that the desired mass splitting  $\delta m$  can be generated by the standard see-saw contribution with  $M_R \sim 10^{13}$  GeV [82].

The effective Majorana mass  $m_{ee} \approx m_0$  is at the level of upper bound from the  $\beta\beta_{0\nu}$  – decay .

The mass  $m_{ee}$  can be suppressed [83] if the electron flavor has large admixture in  $\nu_1$  and  $\nu_2$  , so that the solar neutrino problem is solved by the large mixing MSW solution. Now the effective Majorana mass equals  $m_{ee} \approx m_0(1 - \sin^2 2\theta)$ , and for  $\sin^2 2\theta = 0.7$  one gets suppression factor 0.3. However simple formula (89) does not work [83].

No observable signals are expected in CHORUS/NOMAD and LSND/KARMEN.

### 5.4 “Solar + Atmospheric neutrinos”

Another possibility (fig.8) is to sacrifice the HDM assuming (if needed) that some other particles (*e.g.* sterile neutrinos, axino etc..) are responsible for structure formation in the Universe. In this case  $m_3 \sim 0.1$  eV and  $\nu_\mu - \nu_\tau$  oscillations explain the atmospheric neutrino deficit. Strong  $\nu_\mu - \nu_\tau$  mixing, could be related to relatively small mass splitting between  $m_2$  and  $m_3$  which implies an enhancement of the mixing in the neutrino Dirac mass matrix [84]. It could be related to the see-saw enhancement mechanism [85, 86] endowed by renormalization group enhancement [86] or with strong mixing in charge lepton sector [87].

### 5.5 More neutrino states?

The safe way to accommodate all the anomalies is to introduce new neutrino state (see *e.g.* [88], [89], [90]). As follows from LEP bound on the number of neutrino species (4) this state should be sterile (singlet of SM symmetry group).

Nucleosynthesis bound is satisfied, if  $S$  has the parameters needed for a solution of the solar neutrino problem. In this case one can write the following “scenario” [81] – [98] (fig. 9).

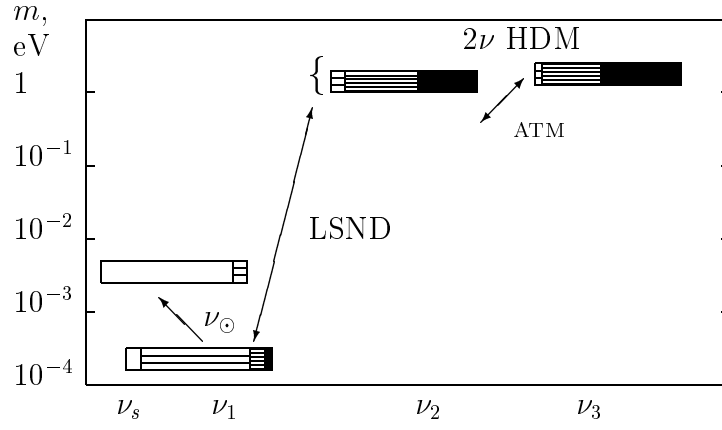


Fig. 9. The same as in fig. 6 for the scenario with sterile neutrino for the solar neutrino problem. The admixture of the sterile neutrino is shown by white regions in boxes.

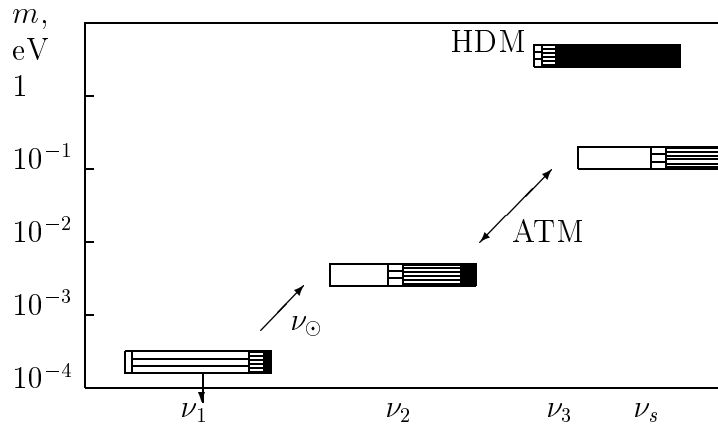


Fig. 10. The same as in fig. 9 for the scenario with sterile neutrino for the atmospheric neutrino problem.

- Sterile neutrino has the mass  $m_S \sim (2 - 3) \cdot 10^{-3}$  eV and mixes with  $\nu_e$ , so that the resonance conversion  $\nu_e - \nu_s$  solves the solar neutrino problem.
- Masses of  $\nu_\mu$  and  $\nu_\tau$  are in the range 2 - 3 eV, they supply the hot component of the DM.
- $\nu_\mu$  and  $\nu_\tau$  form the pseudo Dirac neutrino with large (maximal) mixing and the oscillations  $\nu_\mu - \nu_\tau$  explain the atmospheric neutrino problem.
- $\nu_e$  is very light:  $m_1 < 2 \cdot 10^{-3}$  eV. The  $\bar{\nu}_\mu - \bar{\nu}_e$  mixing can be strong enough to explain the LSND result.
- No effect is expected for  $\nu_\mu - \nu_\tau$  oscillations in CHORUS/NOMAD as well as in future searches of the  $\beta\beta_{0\nu} - decay$ .
- Production of heavy elements in supernova via “r-processes” is problematic for this scenario.

### 5.6 Rescue the standard scenario

The atmospheric neutrino deficit is the problem for the standard scenario. To solve the atmospheric neutrino problem one can assume that an additional light singlet fermion exists with the mass  $m \sim 0.1$  eV. This singlet mixes mainly with muon neutrino, so that  $\nu_\mu - \nu_s$  oscillations explain the data [91]. In this case one arrives at the scheme (fig. 10). Production of  $\nu_s$  singlets in the Early Universe can be suppressed (if needed) by generation of the lepton asymmetry [92] in the  $\nu_\tau - \nu_s$  and  $\bar{\nu}_\tau - \bar{\nu}_s$  oscillations [93].

The presence of large admixture of the sterile component in  $\nu_2$  influences resonance conversion of solar  $\nu_e$ , and also can modify the  $\nu_\mu - \nu_\tau$  oscillations.

There is a number of different mechanisms of neutrino mass generation. All of them contain new free parameters and typically by fitting these parameters one can reproduce the same pattern of the neutrino masses and mixing. Therefore, as much as possible complete information about the pattern of neutrino masses and mixing and also additional information from other sectors of the theory may help in identification of origin of the neutrino mass.

## 6. CONCLUSIONS

1. A number of experimental results indicate that neutrino oscillations or/and resonance flavor conversion really exist. The oscillations and conversion imply (in the simplest version) non-zero neutrino masses and lepton mixing.
2. The most strong indication comes probably from studies of the solar neutrino fluxes. The astrophysical solutions of the solar neutrino problem are strongly disfavored, whereas solutions based on nonzero neutrino mass and mixing give very good fit of the experimental results.
3. New and forthcoming experiments (SuperKamiokande, SNO, accelerator experiments CHORUS and NOMAD, reactor experiments CHOOZ etc.) have a good chance to establish an existence of non-zero neutrino mass and mixing.
4. Different patterns of neutrino masses and mixing have been elaborated which agree with existing constraints and allow one to describe simultaneously some (or even all) neu-



trino anomalies.

5. The patterns will be seriously checked in new and forthcoming experiments. Establishing of the true pattern may shed some light on the origin of neutrino mass.

## REFERENCES

- [1] Particle Group Data, Phys. Rev. D54 (1996) 1.
- [2] M. Gell-Mann, P. Ramond, R. Slansky, in Supergravity, ed. by F. van Nieuwenhuizen and Freedman (Amsterdam, North Holland, 1979) 315; T. Yanagida, in Proc. of the workshop on the unified Theory and Baryon Number in the Universe, eds. O. Sawada and A. Sugamoto (KEK, Tsukuba, 1979) 95.
- [3] R. Mohapatra and G. Senjanović, Phys. Rev. Lett. 44 (1980) 912.
- [4] A. Yu. Smirnov and G. T. Zatsepin, Mod. Phys. Lett. A7 (1992) 1273.
- [5] See for review S. Sarkar, Rep. on Progress in Physics, 59 (1996) 1.
- [6] A. I. Belevsev et al., Phys. Lett. 350 (1995) 263., V. Lobashev, Talk given at XVII Int. Conf. on Neutrino Physics and Astrophysics, Helsinki, Finland, June 1996.
- [7] Ch. Weinheimer et al., Phys. Lett. B300 (1993) 210.
- [8] K. Assamagan et al., Phys. Lett. B335 (1994) 231.
- [9] D. Buskulic et al., Phys. Lett. B349 (1995) 585, A. Gregorio, Talk given at XVII Int. Conf. on Neutrino Physics and Astrophysics, Helsinki, Finland, June 1996.
- [10] G. Gyuk and M. S. Turner, Nucl. Phys. B (Proc. Suppl.) 38 (1995) 18.
- [11] A. Balysh et al., Phys. Lett. B356 (1995) 450. M. Günther et al., Phys. Rev. D55 (1997) 54.
- [12] A. Standt, K. Muto and H.V. Klapdor-Kleingrothaus, Europh. Lett. 13 (1990) 31.
- [13] E. Fischbach, hep-ph/9603396.
- [14] G. Feinberg and J. Sucher, Phys. Rev, **166** (1968) 1638.
- [15] A. Abada, M. B. Gavela and O. Péne, Phys. Lett. B387 (1996) 315.
- [16] A. Loeb, Phys. Rev. Lett. **64** (1990) 115.
- [17] A. Yu. Smirnov and F. Vissani, IC/96/67, hep-ph 9604443.
- [18] S. P. Mikheyev and A. Yu. Smirnov, Sov. Phys. Usp., **30** (1987) 759 and Prog. Part. Nucl. Phys. **23** (1989) 41.
- [19] T. K. Kuo and J. Pantaleone, Rev. Mod. Phys. **59** (1987) 617.
- [20] See for example H. Lipkin, Phys. Lett., **B348** (1995) 604; T. Goldman, hep-ph/9604357. E. Alfinito et al., hep-ph/9510213; Y. Grossman and H. J. Lipkin hep-ph/9607201; W. Grimus and P. Stockinger, Phys. Rev. **D54** (1996) 3414; K. Kiers and S. Nussinov, hep-ph/9506271.
- [21] J. N. Bahcall, Neutrino Astrophysics (Cambridge University Press) Cambridge, England (1989).
- [22] J. N. Bahcall and M. M. Pinsonneault, Rev. Mod. Phys. 64 (1992) 885, ibidem 67 (1995) 1.
- [23] S. Turck-Chieze et al., Phys. Rep. 230 (1993) 57.
- [24] R. Davis, Prog. Part. Nucl. Phys., 32 (1994) 13; K. Lande, Talk given at XVII Int. Conf. on Neutrino physics and Astrophysics, Helsinki, Finland, June 1996.

- [25] Y. Fukuda et al, ICRR-Report-372-96-23, to be published in Phys. Rev. Lett. .
- [26] V. Gavrin, Talk given at XVII Int. Conf. on Neutrino Physics and Astrophysics, Helsinki, Finland, June 1996.
- [27] GALLEX collaboration, P. Anselmann et al., Phys. Lett., B357 (1995) 232; Phys. Lett. B342 (1995) 440; W. Hampel, Phys. Lett. B388 (1996) 384.
- [28] I. Barabanov, (1988) unpublished.
- [29] J. N. Bahcall and H. A. Bethe, Phys. Rev. Lett., 65 (1990) 2233; Phys. Rev. D47 (1993) 1298.
- [30] M. Spiro and D. Vignaud, Phys. Lett. B 242 (1990) 279. 645.
- [31] V. Castellani, S. Degl'Innocenti and G. Fiorentini, Phys. Lett. B 303 (1993) 68; Astron. Astroph. 271 (1993) 601.
- [32] H. Hata, S. Bludman and P. Langacker, Phys. Rev. D 49 (1994) 3622.
- [33] V. S. Berezinsky, Comm. Nucl. Part. Phys. 21 (1994) 249.
- [34] A. Yu. Smirnov, Report DOE/ER/40561-136 -INT94-13-01.
- [35] W. Kwong and S. P. Rosen, Phys. Rev. Lett., 73 (1994) 369.
- [36] S. Parke, Phys. Rev. Lett. 74 (1995) 839.
- [37] S. Degl'Innocenti, G. Fiorentini and M. Lissia, Ferrara preprint INFNFE-10-94.
- [38] N. Hata and P. Langacker, Phys. Rev. D 50 (1994) 632.
- [39] For latest discussion see e.g., N. Hata and P. Langacker, Phys. Rev. D52 (1995) 420.
- [40] P. I. Krastev and A. Yu. Smirnov, Phys. Lett. B 338 (1994) 282.
- [41] V. S. Berezinsky, G. Fiorentini and M. Lissia, Phys. Lett., B 341 (1994) 38.
- [42] W. Kwong and S. P. Rosen, Mod. Phys. Lett. A10 (1995) 6159.
- [43] J. N. Bahcall and P. I. Krastev, Phys. Rev. D53 (1996) 4211.
- [44] J. N. Bahcall M. Fukugita and P. I. Krastev, Phys. Lett. B374 (1996) 1.
- [45] A. Yu Smirnov Talk given at XVII Int. Conf. on Neutrino Physics and Astrophysics, Helsinki, Finland, June 1996, hep-ph 9611435.
- [46] V. N. Gribov and B. M. Pontecorvo, Phys. Lett. 28, (1967) 493;
- [47] Z. G. Berezhiani and A. Rossi, Phys. Rev. D51 (1995) 5229.
- [48] P. I. Krastev and S. T. Petcov, Nucl. Phys. B449 (1995) 605.
- [49] P. I. Krastev and S. T. Petcov, Phys. Rev. D53 (1996) 1665.
- [50] E. Calabresu et al., Astropart. Phys. 4 (1995) 159.
- [51] A. Yu. Smirnov, D. N. Spergel and J. N. Bahcall, Phys. Rev. D49 (1994) 1389.
- [52] S. P. Mikheyev and A. Yu. Smirnov, Sov. J. Nucl. Phys. 42 (1985) 913, Sov. Phys. JETP 64 (1986) 4; L. Wolfenstein, Phys. Rev. D17 (1978) 2369.
- [53] see e.g. X. Shi and D. Schramm, Phys. Lett., B283 (1992) 305; X. Shi, D. Schramm, J. Bahcall, Phys. Rev. Lett. 69 (1992) 717.
- [54] A. Yu. Smirnov, Proc. of the Int Symposium on Neutrino Astrophysics, Takayama/Kamioka 19 - 22 October 1992, ed. by Y. Suzuki and K. Nakamura, p. 105.
- [55] A. S. Joshipura and P. I. Krastev, Phys. Rev. D50 (1994) 3484.
- [56] E. Ma and J. Pantaleone, Preprint UCRHEP-T140 (March 1995);
- [57] G.L. Fogli, E. Lisi and D. Montanino, Phys. Rev. D54 (1996) 2048.
- [58] Y. Totsuka, Nucl. Phys. B (Proc. Suppl.) 31 (1993) 428.
- [59] T. K. Gaisser, Talk given at XVII Int. Conf. on Neutrino Physics and Astrophysics, Helsinki, Finland, June 1996, hep-ph 9611435.

- [60] Y. Fukuda et al, Phys. Lett. B335 (1994) 237.
- [61] P. Litchfield, paper presented at 28th Int. Conf. on High Energy Physics, Warsaw, July 1996.
- [62] O. G. Ryazhskaya, JETP Lett. 60 (1994) 617; ibidem 61 (1995) 237.
- [63] Y. Fukuda et al, Phys. Lett. B388 (1996) 379.
- [64] G. L. Fogli and E. Lisi, Phys. Rev D52 (1995) 2775.
- [65] B. Achkar et al., Nucl. Phys. B434 (1995) 503.
- [66] G. S. Vidyakin et al., JETP Lett., 59 (1994) 364.
- [67] N. N. Chugai, Pis'ma Astron. Zh. **10** (1984) 210; O. F. Dorofeyev, V. N. Rodionov and I. M. Ternov, Sov. Astron. Lett. **11** (1985) 302; A. Vilenkin, Astrophys. J. **451** (1995) 700.
- [68] A. Kusenko and G. Segre, Phys. Rev. Lett. **77** (1996) 4872.
- [69] see E.W. Kolb and M.S. Turner, *The Early Universe*, (Addison-Wesley, New York, 1990).
- [70] E. L. Wright et. al., Astroph. J. 396 (1992) L13, P. Davis, F. J. Summers and D. Schlegel, Nature 359 (1992) 393, R. K. Schaefer and Q. Shafi, Nature 359 (1992) 199, J. A. Holtzman and J. R. Primack, Astroph. J., 405 (1993) 428.
- [71] J. R. Primack, J. Holtzman, A. Klypin, and D. O. Caldwell, Phys. Rev. Lett. 74 (1995) 2160.
- [72] K. S. Babu, R. K. Schaefer, Q. Shafi, Phys. Rev. D53 (1996) 606.
- [73] B. Armbruster et al., Nucl. Phys. (Proc. Suppl.) B38 (1995) 235.
- [74] C. Athanassopoulos et al., Phys. Rev. Lett. 75 (1995) 2650 ibidem 77 (1996) 3082.
- [75] J. Hill, Phys. Rev. Lett. 75 (1995) 2654.
- [76] A. Yu. Smirnov, Nucl. Phys. B466 (1996) 25.
- [77] M. Fukugita and T. Yanagida, Phys. Lett., B174 (1986) 45.
- [78] Y. -Z. Qian et al., Phys. Rev. Lett., 71 (1993) 1965.
- [79] S. Dimopoulos, L. J. Hall and S. Raby, Phys. Rev. D47 (1993) R3697. H.-C. Cheng, M. S. Gill and L. J. Hall, LBL-33936, UCB-PTH-93/11.
- [80] K. S. Babu, J.C. Pati and F. Wilczek, Phys. Lett. B359 (1995) 351.
- [81] D. O. Caldwell and R. N. Mohapatra, Phys. Rev. D48 (1993) 3259.
- [82] S. T. Petcov and A. Yu. Smirnov, Phys. Lett., B322 (1994) 109; A. Joshipura, Z. Phys. C64 (1994) 31; D. O. Caldwell and R. N. Mohapatra, Phys. Rev D50 (1994) 3477; A. Ioannissyan and J. W. F. Valle, Phys. Lett. B332 (1994) 93; B. Bamert and C. P. Burgess, Phys. Lett. B329 (1994) 289; D. G. Lee and R. N. Mohapatra, Phys. Lett. B329 (1994) 463; A. S. Joshipura Phys. Rev. D51 (1995) 1321.
- [83] S. Nussinov and R. N. Mohapatra Phys. Lett. B346 (1995) 75.
- [84] M. Fukugita, M. Tanimoto and T. Yanagida, Prog. Theor. Phys. 89 (1993) 263.
- [85] A. Yu. Smirnov, Phys. Rev D48 (1993) 3264.
- [86] M. Tanimoto, Phys. Lett., 345B (1995) 477; Preprint-EHU-95-8.
- [87] G. K. Leontaris, S. Lola, C. Scheich and D. Vergados Phys. Rev. D53 (1996) 6381.
- [88] J. Peltoniemi and J. W. F. Valle, Nucl. Phys. B406 (1993) 409.
- [89] J. Peltoniemi, D. Tommasini and J. W. F. Valle, Phys. Lett. B298 (1993) 383.
- [90] J. T. Peltoniemi, Mod. Phys. Lett. A8 (1993) 3593.
- [91] E. Akhmedov, P. Lipari and M. Lusignoli, Phys. Lett. B300 (1993) 128.
- [92] R. Foot and R. Volkas, Phys. Rev. Lett. 75 (1995) 4350.

- [93] R. Foot, M. J. Thomson, R.R. Volkas, Phys. Rev. D53 (1996) 5349.
- [94] E. Ma, Preprint UCRHEP-T149.
- [95] R. Foot, R. Volkas, Phys. Rev. D52 (1995) 6595. Z.G. Berezhiani and R. N. Mohapatra, Phys. Rev. D52 (1995) 6607.
- [96] E. J. Chun, A. S. Joshipura and A. Yu. Smirnov, Phys. Lett. B357 (1995) 371.
- [97] E. J. Chun, A. S. Joshipura and A. Yu. Smirnov, Phys. Rev. D54 (1996) 4654.
- [98] E. Ma and P. Roy, preprint UCRHEP-T145 (hep-ph/9504342).